Trapping of an electron in coupled quantum dots in graphene

Prabath Hewageegana*
Department of Physics, University of Kelaniya, Kelaniya 11600, Sri Lanka

Vadym Apalkov†
Department of Physics and Astronomy, Georgia State University, Atlanta, Georgia 30303, USA

(Received 30 July 2008; revised manuscript received 9 February 2009; published 13 March 2009)

Due to Klein's tunneling the electronic states of a quantum dot in graphene have finite widths and an electron in quantum dot has a finite trapping time. This property introduces a special type of interdot coupling in a system of many quantum dots in graphene. The interdot coupling is realized not as a direct tunneling between quantum dots but as coupling through the continuum states of graphene. As a result the interdot coupling modifies both the positions and the widths of the energy levels of the quantum dot system. We study the system of quantum dots in graphene theoretically by analyzing the complex energy spectra of the quantum dot system. We show that in a double-dot system some energy levels become strongly localized with an infinite trapping time. Such strongly localized states are achieved only at one value of the interdot separation. We also study a periodic array of quantum dots in graphene within a tight-binding mode for a quantum dot system. The values of the hopping integrals in the tight-binding model are found from the expression for the energy spectra of the double quantum dot system. In the array of quantum dots the states with infinitely large trapping time are realized at all values of interdot separation smaller than some critical value. Such states have nonzero wave vectors.

DOI: 10.1103/PhysRevB.79.115418 PACS number(s): 73.63.Kv, 73.23.−b, 81.05.Uw

I. INTRODUCTION

Electronic properties of elusive purely two-dimensional form of carbon called graphene[1] are being intensively studied since the discovery of the anomalous quantum Hall effect.[2–4] Graphene is a gapless semiconductor, in which the conduction and the valence bands are touching in two inequivalent points, corresponding to two valleys. Due to unique band structure of graphene, the charge carriers are massless chiral fermions,[5] i.e., massless "relativistic" electrons. Such electrons can cross large potential barriers with almost unity probability.[6] This unusual effect is called Klein's paradox[6,7] and is related to the fact that electrons in graphene can have both positive and negative energies. Furthermore, when a propagating electron reaches the potential barrier it penetrates through it and emerges with the negative energy, i.e., in a hole state. Therefore, the Klein's tunneling introduces an efficient escape channel from any trapping potential. As a consequence of this unique property, the control of electron behavior by means of electrical confinement potentials becomes a challenging task.

It also follows from the Klein's paradox that there are no conventional quantum dots in graphene, i.e., quantum dots,[8] which can localize electrons within finite spatial regions. Therefore, from fundamental point of view, it is desirable to find a feasible and controllable way to realize the quantum dot trapping potential for relativistic electrons in graphene. This is particularly important for future electronic applications of graphene in photodetectors,[9] quantum information processing, quantum computers,[10] etc. Since the conventional quantum dots cannot be realized in graphene, we need to consider the spatial confinement potentials, which cannot localize but *trap* an electron for a long enough time. If the trapping time is longer than the time required by a corresponding application, then we can consider the electron in such confinement potential as the localized electron. The trapping of an electron in graphene quantum dots can be achieved by introducing a transverse momentum,[11–13] which is determined by the electron angular momentum[13] in a cylindrically symmetric quantum dot. The transverse momentum introduces an effective electron mass and, as a result, the trapping potential. The width and the height of the trapping potential strongly depend on the electron angular momentum and on the smoothness of the confinement potential.[13] In this case only the electrons with large angular momentum can be trapped by a smooth enough confinement potential.

Another mechanism of electron trapping is due to interference effects.[14,15] The trapping in this case can be realized for the electrons with both large and small angular momenta and for the confinement potential with both smooth and sharp boundaries. The trapping properties of the potential becomes very sensitive to the whole structure of the confinement. If the confinement potential satisfies special conditions[15] then the electron can be strongly localized, i.e., the trapping time is infinitely large.

One of the directions of conventional quantum dot research is related to coupled quantum dots, i.e., "artificial molecules." The coupled quantum dots have been proposed as building blocks of quantum computing.[16] Recently the problem of coupled quantum dots in graphene has been addressed in the literature.[17] In this relation it is very important to understand the trapping properties of the coupled quantum dots. In the present paper we address this problem. We consider the effect of the coupling of quantum dots on the electron trapping time.

In the conventional coupled quantum dot systems[18] there are two types of interdot coupling. The first one is a direct interdot tunneling, which shifts the energy levels of the individual quantum dots. The second type of coupling is realized in systems, where the states of the quantum dots are degen-

erate with the continuum states, e.g., the continuous states of the leads in resonant tunneling experiments.[19,20] In this case the states of the quantum dots have finite widths, which are the widths of the tunneling conductance maxima. Then the second type of coupling is the coupling through the continuum states of the leads. This type of coupling has interference nature and affects the width of the quantum dot levels.[20] As a result some levels of the coupled quantum dots become narrow and the other levels become broad. Therefore in the conventional quantum dot systems, the real part of the interdot coupling matrix elements are determined by the direct interdot tunneling, while the imaginary part is due to coupling through the continuum states.

In the graphene quantum dot system there is no direct tunneling between two spatially separated quantum dots. The levels of the quantum dots in graphene are degenerate with the continuum states. Therefore the interdot coupling in graphene should be described as the coupling through its continuum states. In this case the coupling matrix elements have both real and imaginary parts, and we should expect that the interdot coupling in graphene affects both the position and the width, i.e., the electron escape rate, of the levels of the dot system. We show below that the interdot coupling in graphene can result in strong suppression of the escape rates from the dot system and under some conditions the escape rate can be even zero. This suppression is the result of interference effect and is sensitive to the shape of the confinement potential. Below we discuss the properties of the trapped states in a double quantum dot system and in periodic array of quantum dots.

The trapped states or decaying states of the quantum dot system are revealed as peaks, i.e., resonances, in the scattering cross section or as the first-order poles of the scattering matrix in the complex energy plane. The poles are complex, where the real part corresponds to the energy of the resonance and the inverse of the imaginary part describes the lifetime of the decaying state. In the present paper we use different approach to the problem of resonances, i.e., trapped states, of the quantum dot system. This approach was originally introduced by Gamow in Ref. 21. In this approach the resonances are described by eigenfunctions, Gamow's vectors, with complex eigenvalues. The real part of the complex eigenvalue is associated with the energy of the resonance, and the inverse of the imaginary part of the eigenenergy is associated with the lifetime of the decaying state. Therefore the resonances in this approach have complex energy and are considered as the long-lived states in the decay process.[22] Such states can be found as the time-independent solutions of the Schrödinger equation with purely outgoing boundary conditions. The stationary solutions with such boundary conditions exist only at complex eigenenergies.

The paper is organized as follows. In Secs. II and III we discuss the double quantum dot system in graphene. In Sec. II we introduce the main system of equations, which determines the complex energy spectra of the double-dot system. The system of equations is solved numerically. The results of calculations and the discussion of the results are presented in Sec. III. In Sec. IV we consider a periodic array of quantum dots and introduce the tight-binding model, which describes the periodic system of quantum dots. Within the tight-binding model we obtain the complex energy spectrum of the array of quantum dots.

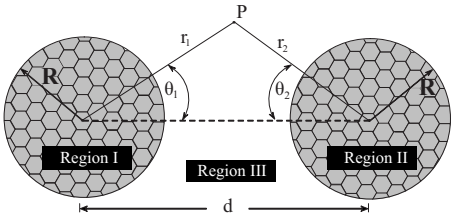

FIG. 1. The geometry of the coupled graphene quantum dots. The quantum dots have the same radius R. Here d is the distance between the centers of the quantum dots (interdot distance). To characterize the position of point P we introduce the polar coordinates r_1, θ_1 and r_2, θ_2 for each quantum dot.

II. DOUBLE QUANTUM DOT SYSTEM: MAIN EQUATIONS

The coupled quantum dots system is shown schematically in Fig. 1. We consider two identical cylindrically symmetric quantum dots, which are characterized by radius R. The distance between the centers of the quantum dots is d. Then the system under consideration consists of three regions: region I (quantum dot 1), region II (quantum dot 2), and region III (see Fig. 1). To describe the system it is convenient to introduce the polar coordinates for each quantum dot: r_1 and θ_1 for the first quantum dot and r_2 and θ_2 for the second quantum dot (see Fig. 1). We assume that the quantum dots have sharp boundaries[14,15] and the corresponding confinement potential has the following form:

$$V(\vec{r}) = \begin{cases} -V_1 & \text{if } r_1 < R \quad \text{region I} \\ -V_2 & \text{if } r_2 < R \quad \text{region II} \\ 0 & \text{if } r_1, r_2 > R \quad \text{region III}, \end{cases} \tag{1}$$

where $V_1, V_2 > 0$.

With the confinement potential [Eq. (1)] the Hamiltonian of a single electron in graphene is given by an expression[5,23]

$$\mathcal{H} = \frac{\gamma}{\hbar}(\vec{\sigma} \cdot \vec{p}) + V(\vec{r}), \tag{2}$$

where $\vec{\sigma}$ are the Pauli matrices, $\vec{p} = -i\partial/\partial\vec{r}$, and $\gamma = \sqrt{3}a_0\gamma_0/2$ is the band parameter. Here $a_0 = 0.246$ nm is the lattice constant and $\gamma_0 \approx 3.03$ eV is the transfer integral between the nearest-neighbor carbon atoms.[24] In expression (2) for the Hamiltonian of the system we consider a single valley only, taking into account that the energy spectrum is a double valley degenerate. In addition to the valley degeneracy each level has double spin degeneracy. Therefore, each energy level, we discuss below, has a fourfold degeneracy.

We define the trapped states of the quantum dot system as the long-lived states in the decay process.[22] In this case the trapped states of the system is the time-independent solution of the Schrödinger equation, which is characterized by the outgoing boundary conditions at infinity and a complex energy, E. The escape rate from the quantum dots and the trapping time of the corresponding state are determined by the

imaginary part of the energy. For example, the trapping time is $\tau=\hbar/\mathrm{Im}[E]$, where $\mathrm{Im}[E]$ is imaginary part of the energy of the level and $\hbar$ is the reduced Planck constant. Within this approach the solution of the Schrödinger equation in region III should have only outgoing waves.

To find the solution of the Schrödinger equation corresponding to Hamiltonian (2) we introduce the basis states, which have the same form as single quantum dot states.[15] The form of the wave function corresponding to a single quantum is described in Appendix A and in Ref. 15. Then the general solution of the Schrödinger equation for the double-dot system has the following form:

$$\psi_{\mathrm{I}}(r_1,\theta_1)=\sum_m A_m\begin{pmatrix} J_{|m-1/2|}(\varepsilon_1 r_1/R)e^{i(m-1/2)\theta_1} \\ iJ_{|m+1/2|}(\varepsilon_1 r_1/R)e^{im\theta_1}\end{pmatrix} \tag{3}$$

in region I ($r_1<R$), where $\varepsilon_1=R(E+V_1)/\gamma$ and J_n is the Bessel function of the nth order;

$$\psi_{\mathrm{II}}(r_2,\theta_2)=\sum_m C_m\begin{pmatrix} J_{|m-1/2|}(\varepsilon_2 r_2/R)e^{i(m-1/2)\theta_2} \\ iJ_{|m+1/2|}(\varepsilon_2 r_2/R)e^{im\theta_2}\end{pmatrix} \tag{4}$$

in region II ($r_2<R$), where $\varepsilon_2=R(E+V_2)/\gamma$, and

$$\psi_{\mathrm{III}}(r_1,r_2,\theta_1,\theta_2)=\sum_m B_m\begin{pmatrix} H_{|m-1/2|}(\varepsilon r_1/R)e^{i(m-1/2)\theta_1} \\ iH_{|m+1/2|}(\varepsilon r_1/R)e^{im\theta_1}\end{pmatrix} + \sum_m D_m\begin{pmatrix} H_{|m-1/2|}(\varepsilon r_2/R)e^{i(m-1/2)\theta_2} \\ iH_{|m+1/2|}(\varepsilon r_2/R)e^{im\theta_2}\end{pmatrix} \tag{5}$$

in region III ($r_1,r_2>R$), where $\varepsilon=RE/\gamma$ and H_n is the Hankel function of the nth order of the first kind. Here $m=\pm 1/2,\pm 3/2,\ldots$ is an orbital angular momentum, defined for each quantum dot separately. In these expressions we took into account that the wave function should be finite at $r_1=r_2=0$ and outside the quantum dot system we have outgoing waves.

The wave function should be continuous at the boundary between regions I and III ($r_1=R$) and at the boundary between regions II and III ($r_2=R$). The continuity condition, for example, at the boundary between regions I and III have the form

$$\psi_{\mathrm{I}}(R,\theta_1)=\psi_{\mathrm{III}}[R,r_2(\theta_1),\theta_1,\theta_2(\theta_1)], \tag{6}$$

where

$$r_2(\theta_1)=\sqrt{R^2+d^2-2dR\cos\theta_1},$$

$$\theta_2(\theta_1)=\sin^{-1}\left[\frac{R\sin\theta_1}{r_2(\theta_1)}\right]. \tag{7}$$

Taking into account expressions (3) and (5) for the wave function in the regions I and III and integrating boundary condition (6) over the boundary surface, we obtain the following equation:

$$\frac{J_{|m-1/2|}[\varepsilon+\nu_1]}{J_{|m+1/2|}[\varepsilon+\nu_1]}=\frac{B_m H_{|m-1/2|}[\varepsilon]+\sum_{m'} D_{m'}\Gamma^{(-)}_{m,m'}}{B_m H_{|m+1/2|}[\varepsilon]+\sum_{m'} D_{m'}\Gamma^{(+)}_{m,m'}}. \tag{8}$$

The similar equation can be derived from the continuity condition at the boundary between regions II and III,

$$\frac{J_{|m-1/2|}[\varepsilon+\nu_2]}{J_{|m+1/2|}[\varepsilon+\nu_2]}=\frac{\sum_{m'} B_{m'}\Gamma^{(-)}_{m,m'}+D_m H_{|m-1/2|}[\varepsilon]}{\sum_{m'} B_{m'}\Gamma^{(+)}_{m,m'}+D_m H_{|m+1/2|}[\varepsilon]}, \tag{9}$$

where $\nu_1\equiv RV_1/\gamma$, $\nu_2\equiv RV_2/\gamma$, and

$$\Gamma^{(\pm)}_{m,m'}=\int_0^{2\pi} H_{|m'\pm 1/2|}\left[\frac{\varepsilon r_2(\theta_1)}{R}\right] \times e^{-i[(m\pm 1/2)\theta_1-(m'\pm 1/2)\theta_2(\theta_1)]}d\theta_1. \tag{10}$$

The solution of the system of Eqs. (8) and (9) determines the complex energy of the electronic states in the double quantum dot system, where the coefficients $\Gamma^{(\pm)}_{m,m'}$ describe the interdot coupling. In the limit of large interdot separation, d, the interdot coupling terms become small and Eqs. (8) and (9) transform into eigenvalue equations for two uncoupled single quantum dots.[15] At finite interdot separation the coefficients $\Gamma^{(\pm)}_{m,m'}$ introduce the coupling between the states with different angular momentum, m. In Eqs. (8) and (9) the summation runs over all possible values of angular momentum, m'. Below we consider the small values of angular momentum, m, and to make the system of Eqs. (8) and (9) finite we restrict the values of m in Eqs. (8) and (9) by inequality: $|m|\leq 5/2$. Under this restriction we solve the system of Eqs. (8) and (9) numerically to find the complex energy spectra of the double-dot system.

III. DOUBLE QUANTUM DOT SYSTEM: RESULTS AND DISCUSSION

At large interdot separation the interdot coupling is small and the double quantum dot system becomes the system of uncoupled quantum dots. The energy spectra of each of the quantum dots is determined from the eigenvalue equation,[15]

$$\frac{J_{|m-1/2|}(\varepsilon+\nu)}{J_{|m+1/2|}(\varepsilon+\nu)}=\frac{H_{|m-1/2|}(\varepsilon)}{H_{|m+1/2|}(\varepsilon)}. \tag{11}$$

This equation can be obtained from Eqs. (8) and (9) at zero interdot coupling, $\Gamma^{(\pm)}_{m,m'}=0$. The solution of this equation is a complex energy spectrum, where the imaginary part of the energy determines the electron trapping time in the quantum dot. For identical quantum dots, i.e., $\nu=\nu_1=\nu_2$, the energy spectra of two quantum dots become degenerate. At finite interdot separation we should expect the splitting of the degenerate energy levels. Since the coefficients $\Gamma^{(\pm)}_{m,m'}$, which determines the interdot coupling, are complex then the finite interdot coupling modifies both the real and imaginary parts of the electron energy.

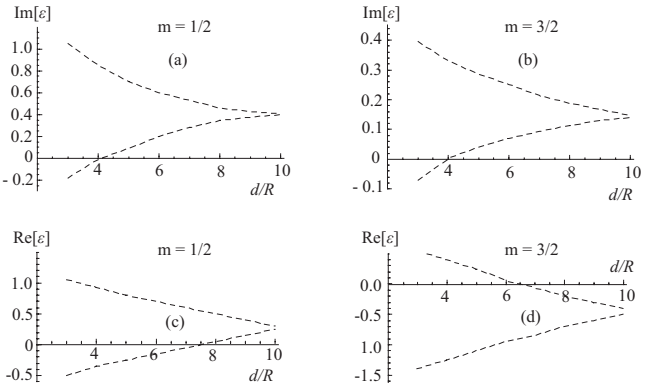

FIG. 2. [(a) and (b)] The imaginary parts of the energies, Im[ε], of the quasilocalized states are shown as functions of d/R for double quantum dot system in graphene for different values of angular momentum, m, (as indicated). [(c) and (d)] Same diagram for the real part of the energy, Re[ε]. For all the panels $\nu_1=\nu_2=20$. The lifetime of the trapped state is determined by the inverse of the absolute value of the imaginary part of the complex energy.

To describe the effect of interdot coupling on the trapping properties of the double quantum dot system, we trace the splitting of the degenerate levels of double quantum dots with decreasing the interdot separation, d. We characterize the states at finite values of d by the angular momentum of the original quantum dot states at large interdot separation. The results of calculations are shown for the angular momenta $m=1/2$ and $m=3/2$ in Fig. 2. For each value of m we show only one set of energy levels, which corresponds to the lowest escape rate, i.e., the lowest imaginary part of the energy, at large interdot separation.

We can see from Fig. 2 that at finite interdot separation, d, the interdot coupling introduces the splitting of the degenerate energy levels of the double-dot system. The splitting occurs both for the real and imaginary parts of the energy. The escape from one of the states of the double quantum dots is suppressed, i.e., the imaginary part of the energy decreases. The most important property of this dependence is that at finite value of d, $d\approx 4R$, the imaginary part of the energy becomes zero. It means that the electron at this level becomes strongly localized, i.e., the trapping time is infinitely large. In addition to suppression of the escape rate from one of the levels of the double-dot system we can see an enhancement of the escape rate from another level. This fact illustrates the splitting of the degenerate levels due to interdot coupling. The splitting of the real part of the energies has almost linear dependence on the interdot separation, d.

In Fig. 2 the states with positive and negative imaginary parts are shown. In general, the solutions of the eigenenergy equation, which describes the Gamow's states, always come in complex conjugate pairs. One of the states in this pair corresponds to the decaying state, and another state describes the growing state. In physical applications we are interested only in the decaying states. In Fig. 2 we show only one set of energies, which has smooth dependence on the parameters of the system. We also have complex conjugate set of energies, which is not shown in the figure. The energies shown in Fig. 2 have both positive and negative imaginary parts. In this case to define the lifetime of the trapped state we need to consider the absolute value of the imaginary part of the energy. Namely, the lifetime is determined by the inverse of the absolute value of the imaginary part.

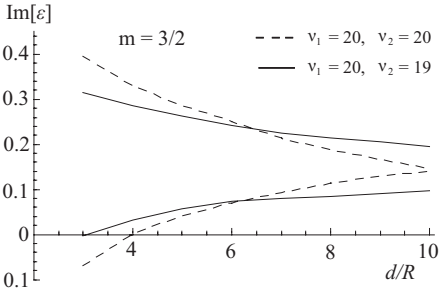

FIG. 3. The imaginary parts of the energies, Im[ε], of the quasilocalized states are shown as functions of d/R for double quantum dot system for angular momentum, $m=3/2$, and different strength of confinement potentials, ν_1 and ν_2 (as indicated).

The suppression of the escape rate of an electron from the double quantum dot system is due to interference effects. Therefore, this behavior is sensitive to the parameters and the positions of the quantum dots. The exact value of the interdot separation, at which the strongly localized state is realized, depends on the actual structure of the quantum dots.

The results shown in Fig. 2 correspond to the quantum dot system with two identical quantum dots. In this case the interdot coupling has the strongest effect on the electron energy spectra and on the electron trapping time. This is because the energy spectra of two quantum dots at large interdot separation are identical. If the quantum dots have different parameters, e.g., different strength of the confinement potential, then the effect of the interdot coupling is suppressed. The results of calculations for the double quantum dot system with the different values of the confinement potential strength, $\nu_1\neq\nu_2$, are shown in Fig. 3. We can see that at large interdot separation, d, the energies of two quantum dots are different. With decreasing the distance, d, the interdot coupling introduces an additional splitting of the energy levels. The imaginary part of one of the levels of the double-dot system becomes smaller, i.e., the electron in this state becomes more localized. We can see from Fig. 3 that the effect of the interdot coupling on the energy spectra is less than in the case of the identical quantum dots. As a result, the state with zero imaginary part is achieved at smaller values of the interdot separation, $d\approx 3R$.

The data shown in Fig. 3 illustrate the possibility of experimental control of the electron trapping in the quantum dot system. Namely, if we keep the same separation between the dots and change the strength of the confinement potential for one of the dots (ν_1 or ν_2), then we can switch between the states with different trapping times. For example, if the interdot separation is $d\approx 4R$ and we start from the identical quantum dots and then change the confinement potential of one of the dots, then the electron state transforms from the highly trapped to the weakly trapped state.

We can illustrate the finite trapping time of an electron in terms of the widths of the peaks in the electron density of states. The width of the peak is determined by the imaginary

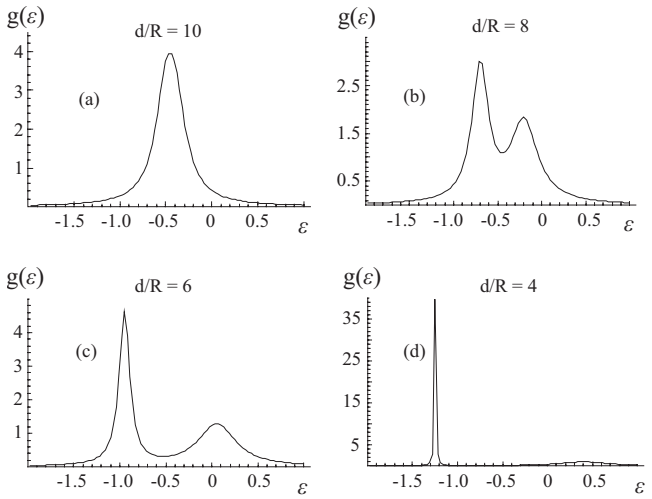

FIG. 4. The density of states, $g(\varepsilon)$ as a function of ε for different values of d/R (as indicated). Here $\nu_1=\nu_2=20$ and $m=3/2$.

part of the energy of the corresponding state. Therefore, the strongly trapped states correspond to sharp peaks in the electron density of states. The density of states can be expressed through the real and imaginary parts of the energies by the following equation:[25]

$$g(\varepsilon)=\frac{1}{\pi}\sum_j \frac{|\mathrm{Im}(\varepsilon_j)|}{[\varepsilon-\mathrm{Re}(\varepsilon_j)]^2+[\mathrm{Im}(\varepsilon_j)]^2}. \tag{12}$$

The density of states is shown in Fig. 4 for the double quantum dot system of identical quantum dots, i.e., $\nu_1=\nu_2=20$. In this figure only the states with $m=3/2$, which correspond to the results shown in Figs. 2(b) and 2(d), are taken into account. At large interdot separations [Fig. 4(a)] there is a broad peak, which corresponds to two degenerate states of the quantum dots. With decreasing the interdot distance, d, the formation of two peak structure is observed. Here the low-energy peak is narrow and the higher-energy peak is broad. Finally at $d/R\approx 4$ the width of the lower-energy peak becomes very small, which illustrates almost zero escape rate of the electron from the double quantum dot system.

IV. ARRAY OF QUANTUM DOTS

In Sec. III we illustrated the appearance of the strongly localized states of the electron in the double quantum dot system. Such states exist only at specific values of the interdot separation. Additional degree of freedom can be introduced into the dot system if we increase the number of coupled quantum dots. One of the examples of such system is the periodic array of identical quantum dots. Such array is characterized by the radius of each quantum dot, R, and the interdot distance, d [see Fig. 5(a)]. Here the interdot distance, d, becomes the period of the quantum dot array system.

At large interdot distance, $d\gg R$, all quantum dots have the same energy spectrum. When the interdot distance decreases the interdot coupling results in splitting of the degenerate energy levels and formation of the band structure. To analyze this energy structure we consider only one electron

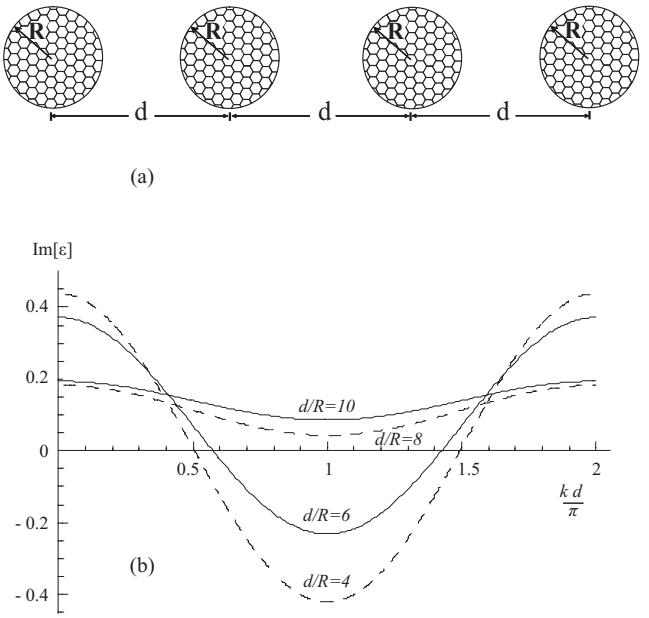

FIG. 5. The imaginary part of the energy, $\mathrm{Im}[\varepsilon]$, is shown as a function of the wave vector k for different values of d/R (as indicated). Here $\nu_0=20$ and $m=3/2$. The lifetime of the trapped state is determined by the inverse of the absolute value of the imaginary part of the complex energy.

state per quantum dot. This state is characterized by the angular momentum, m, and the complex energy, ε_m. We introduce the interdot coupling through the tight-binding model, which is described by the following tight-binding Hamiltonian,

$$\mathcal{H}_t=\sum_i \varepsilon_m a_i^\dagger a_i+\sum_i t_m a_i^\dagger a_{i+1}+\mathrm{H.c.}, \tag{13}$$

where a_i is the annihilation operator of an electron in the state with energy ε_m at the quantum dot i and t_m is the interdot hopping integral. The value of the hopping integral can be found from the application of Hamiltonian (13) to a double-dot system. For the double-dot system the energy spectra is found from the solution of the system of Eqs. (8) and (9). In this system of equations we consider only one level per dot and then compare the corresponding energy spectrum with the energy spectrum of the tight-binding model. This comparison gives the following value for the hopping integral in the tight-binding model,

$$t_m=-\frac{\varepsilon_m\varepsilon_{m,1}}{2m\nu}\frac{\Gamma^{(+)}_{m,m}J_{|m-1/2|}(\varepsilon_{m,1})-\Gamma^{(-)}_{m,m}J_{|m+1/2|}(\varepsilon_{m,1})}{H_{|m+1/2|}(\varepsilon_m)J_{|m-1/2|}(\varepsilon_{m,1})}, \tag{14}$$

where $\varepsilon_{m,1}=R(E_m+V)/\gamma=\varepsilon_m+\nu$. The details of derivation of the hopping integral can be found in Appendix B.

The states of Hamiltonian (13) are characterized by a wave vector, k, and the corresponding energy spectrum has a form

$$\varepsilon(k) = \varepsilon_m + 2t_m \cos(kd), \tag{15}$$

where the wave vector k is defined within the interval $0 \leq k < 2\pi/d$.

Both the energy ε_m and the hopping integral t_m are complex. Then the energy spectrum, $\varepsilon(k)$, of the quantum dot system is complex, and the imaginary part of the energy determines the escape rates of an electron from the quantum dot array.

In Fig. 5(b) the imaginary part of the energy spectrum is shown as a function of the wave vector, k, at $m=3/2$ and different values of the period, d. We can see from the figure that if the period, d, is less than some critical value, $d \lesssim 8R$, then there are always two states with zero imaginary part of the energy, which means that electron trapping time at these states is infinitely large. This property is different from the double quantum dot system, where the state with large trapping time can be realized only at one value of the interdot distance.

The manifestation of the specific behavior of the imaginary part of the energy spectra could be the formation of the charge-density wave in the periodic array of quantum dots in graphene. Indeed, if initially all quantum dots are occupied by electrons, then after some time the electrons at the states with small trapping time will escape from the quantum dot system. Finally, only the states with large trapping times will be occupied. Such states have nonzero momentum and the occupation of these states results in the charge-density wave.

V. CONCLUSION

The unique feature of the quantum dots in graphene is that the discrete electron energy spectra of the quantum dot is degenerate with the continuum spectra of graphene. As a result the states of the quantum dot have finite width and the electrons at these states have finite lifetime. In this case the interdot coupling in the system of many quantum dots in graphene can be described as the combination of the following processes: (i) the electron escapes from a quantum dot into the continuum states of graphene; (ii) then the electron freely propagates outside the quantum dots; (iii) and finally the electron is trapped by another quantum dot. This type of processes introduce interdot coupling, which has both real and imaginary parts. As a result, the interdot coupling changes both the positions and the widths of the energy levels of the quantum dots. For some states of the quantum dot system the width of the energy levels, i.e., the escape rate from the quantum dots, is suppressed and can be even zero. For the double quantum dot system such states with infinitely large trapping time is realized only at one value of the interdot distance. This distance depends on the parameters of the quantum dots, e.g., the radius of the dot, the strength of the confinement potential, and the shape of the quantum dot.

For a periodic array of quantum dots in graphene the interdot coupling results in the band structure of the energy spectra. In this case the strongly localized states with zero width exist at all values of interdot separation smaller than some critical value. The states with infinitely large trapping time have nonzero wave vector.

In the above analysis we assumed that the quantum dots have very special form. Namely, for each quantum dot the confinement potential is cylindrically symmetric with sharp boundaries [see Eq. (1)]. In reality there is always deviation from the cylindrically symmetric shape of the quantum dot, and the confinement potential is always smooth. The fact that the potential is smooth does not affect qualitatively the results we presented above. Even in smooth potential the electron can be strongly localized due to interference of the electron waves within the quantum dot. Similar to the quantum dot with sharp boundary such localization occurs at one energy only and only at special sets of parameters of the confinement potential. Then in the system of coupled quantum dots with smooth boundaries we should expect the same results as for the quantum dots with sharp boundaries. The smoothness of the confinement potential modifies only the quantitative results, e.g., the interdot distance at which the strong trapping is observed in double quantum dot system or the wave vectors at which the strong trapping is observed in the array of quantum dots.

The deviation of the shape of the quantum dot from cylindrically symmetric one introduces an additional escape channels from the quantum dot due to mixture of the states with different angular momentum. In Ref. 15 it was shown that if the radius of the quantum dot changes within the interval $(R-\delta R, R+\delta R)$, e.g., for elliptical quantum dot, then the imaginary part of the energy, which determines the escape rate from the quantum dot, is

$$\mathrm{Im}[\varepsilon] = \frac{\pi}{[(m-1/2)!]^2}\left[1-\frac{1}{2m}\right]^{2m+1}(V_0\delta R/\gamma)^{2m} \tag{16}$$

for $m > 1/2$ and

$$\mathrm{Im}[\varepsilon] = \frac{\pi V_0 \delta R}{\gamma \ln(V_0\delta R/\gamma)} \tag{17}$$

for $m=1/2$. To observe strongly trapped states in a system of coupled quantum dots the imaginary part of the energy of a single dot should be small enough. For example, from Fig. 2 we can conclude that the upper limit for imaginary part of a single dot is around 0.2 for $m=3/2$. Then from Eq. (16) we can find the maximum possible deviation of the quantum dot from the cylindrically symmetric form

$$\delta R \approx 0.7\frac{\gamma}{V_0}. \tag{18}$$

Since $RV_0/\gamma = 20$ then we can express the above value as a relative deviation of the radius of the quantum dot

$$\frac{\delta R}{R} \approx 0.04. \tag{19}$$

For example, if the radius of the quantum dot is 50 nm, then the radius cannot be changed more than by 2 nm.

ACKNOWLEDGMENT

The work was supported by Petroleum Research Fund under Grant No. 43216-G10.

APPENDIX A

The wave function, $\psi(\vec{r})$, corresponding to Hamiltonian (2), is a two-component function.[15] For cylindrically symmetric confinement potential,

$$V(r) = \begin{cases} 0 & \text{if } r > R \\ -V_0 & \text{if } r < R, \end{cases} \tag{A1}$$

where $V_0 > 0$, the two-component wave function has the following form:

$$\psi(r,\theta) = e^{i(m-1/2)\theta}\begin{pmatrix} \chi_1(r) \\ \chi_2(r)e^{i\theta} \end{pmatrix}, \tag{A2}$$

where r and θ are cylindrical coordinates and $m = \pm 1/2, \pm 3/2, \ldots$ is orbital angular momentum. With this form of the wave function the Schrödinger equation, corresponding to the Hamiltonian in Eq. (2), becomes

$$V(r)\chi_1 - i\gamma\frac{d\chi_2}{dr} - i\gamma\frac{m+1/2}{r}\chi_2 = E\chi_1, \tag{A3}$$

$$V(r)\chi_2 - i\gamma\frac{d\chi_1}{dr} + i\gamma\frac{m-1/2}{r}\chi_1 = E\chi_2. \tag{A4}$$

By eliminating χ_1 (or χ_2) in the system of Eqs. (A3) and (A4) we can easily obtain that χ_1 and χ_2 satisfy Bessel's differential equations of the orders of $|m-1/2|$ and $|m+1/2|$ for the functions χ_1 and χ_2, respectively.

Inside the quantum dot the wave function should be finite at the origin, $r=0$. Then the general solution of the system of Eqs. (A3) and (A4) inside the quantum dot, where $V=-V_0$, has the form

$$\begin{pmatrix} \chi_1(r) \\ \chi_2(r) \end{pmatrix} = A\begin{pmatrix} J_{|m-1/2|}[(\varepsilon+\nu_0)r/R] \\ iJ_{|m+1/2|}[(\varepsilon+\nu_0)r/R] \end{pmatrix}, \tag{A5}$$

where J_n is the Bessel function of the nth order, and we introduced the dimensionless energy $\varepsilon = RE/\gamma$ and dimensionless confinement potential $\nu_0 = RV_0/\gamma$.

Outside the quantum dot, i.e., at $r > R$, the solutions of the corresponding Bessel differential equations describe the outgoing waves, $\propto \exp(ikr)$. Therefore at $r > R$, the solution of Eqs. (A3) and (A4) are Hankel functions of the first kind. Then the general solution of the system of Eqs. (A3) and (A4) at $r > R$, where $V=0$, is

$$\begin{pmatrix} \chi_1(r) \\ \chi_2(r) \end{pmatrix} = B\begin{pmatrix} H_{|m-1/2|}(\varepsilon r/R) \\ iH_{|m+1/2|}(\varepsilon r/R) \end{pmatrix}, \tag{A6}$$

where H_n is the Hankel function of nth order of the first kind.

Wave functions (A5) and (A6) should be continuous at the boundary of the quantum dot, $r=R$. From this condition the complex energy spectra of a single quantum dot can be found.[15]

APPENDIX B

To find the hopping integral in the tight-binding model [Eq. (13)] we consider a system of two identical quantum dots with only one state per dot. We assume that the angular momentum of this state is m and the energy is ε_m. In this case in Eqs. (8) and (9), which determine the energy spectrum of the system, we need to keep only the terms with $m' = m$. Then Eqs. (8) and (9) become

$$\frac{J_{|m-1/2|}(\varepsilon+\nu)}{J_{|m+1/2|}(\varepsilon+\nu)} = \frac{B_m H_{|m-1/2|}(\varepsilon) + D_m \Gamma^{(-)}_{m,m}}{B_m H_{|m+1/2|}(\varepsilon) + D_m \Gamma^{(+)}_{m,m}}, \tag{B1}$$

$$\frac{J_{|m-1/2|}(\varepsilon+\nu)}{J_{|m+1/2|}(\varepsilon+\nu)} = \frac{B_m \Gamma^{(-)}_{m,m} + D_m H_{|m-1/2|}(\varepsilon)}{B_m \Gamma^{(+)}_{m,m} + D_m H_{|m+1/2|}(\varepsilon)}, \tag{B2}$$

where $\nu_1 = \nu_2 = \nu$. A nontrivial solution of Eqs. (B1) and (B2) can be found from the condition that the determinant of the following matrix:

$$\boldsymbol{A} = \begin{pmatrix} A_1(\varepsilon) & A_2(\varepsilon) \\ A_2(\varepsilon) & A_1(\varepsilon) \end{pmatrix}, \tag{B3}$$

is zero. Here

$$A_1(\varepsilon) = H_{|m+1/2|}(\varepsilon)J_{|m-1/2|}(\varepsilon+\nu) - H_{|m-1/2|}(\varepsilon)J_{|m+1/2|}(\varepsilon+\nu), \tag{B4}$$

$$A_2(\varepsilon) = \Gamma^{(+)}_{m,m}J_{|m-1/2|}(\varepsilon+\nu) - \Gamma^{(-)}_{m,m}J_{|m+1/2|}(\varepsilon+\nu). \tag{B5}$$

For uncoupled quantum dots the nondiagonal element, A_2, of the matrix is zero and the energy spectrum is determined by equation $A_1(\varepsilon)=0$. This equation gives two degenerate energy levels with the energy equal to the energy of a single quantum dot, $\varepsilon = \varepsilon_m$.

We assume that the interdot coupling is small and the energy of the coupled quantum dots is close to ε_m. Then expanding the diagonal element, $A_1(\varepsilon)$, of the matrix around ε_m, we obtain

$$A_1(\varepsilon) = A_1[(\varepsilon-\varepsilon_m)+\varepsilon_m] \approx A_1(\varepsilon_m) + A_1'(\varepsilon_m)[\varepsilon-\varepsilon_m], \tag{B6}$$

where A_1' is the first derivative of the function. Since $A_1(\varepsilon_m)=0$, then Eq. (B6) becomes

$$A_1(\varepsilon) \approx A_1'(\varepsilon_m)[\varepsilon-\varepsilon_m]. \tag{B7}$$

With this expression the matrix $\boldsymbol{A}$ takes the form

$$\boldsymbol{A} = \begin{pmatrix} A_1'(\varepsilon_m)[\varepsilon-\varepsilon_m] & A_2(\varepsilon_m) \\ A_2(\varepsilon_m) & A_1'(\varepsilon_m)[\varepsilon-\varepsilon_m] \end{pmatrix}. \tag{B8}$$

From the condition that the determinant of the matrix $\boldsymbol{A}$ is zero we can find the energy of the double-dot system,

$$\varepsilon = \varepsilon_m \pm \frac{A_2(\varepsilon_m)}{A_1'(\varepsilon_m)}. \tag{B9}$$

In the tight-binding model [Eq. (13)] of double quantum dot system the energy spectrum is

$$\varepsilon = \varepsilon_m \pm t_m. \tag{B10}$$

Comparing Eqs. (B9) and (B10), we obtain the expression

for the hopping integral in the tight-binding model,

$$t = \frac{A_2(\varepsilon_m)}{A_1'(\varepsilon_m)}. \quad \text{(B11)}$$

Using the properties of Bessel and Hankel functions, we can find the derivative $A_1'(\varepsilon_m)$ in the following form:

$$A_1'(\varepsilon_m) = -\frac{2m\nu}{\varepsilon_m \varepsilon_{m,1}} H_{|m+1/2|}(\varepsilon_m) J_{|m-1/2|}(\varepsilon_{m,1}), \quad \text{(B12)}$$

where $\varepsilon_{m,1} = \varepsilon_m + \nu$. Substituting Eqs. (B5) and (B12) into Eq. (B11), we obtain expression (14) for the hopping integral in the tight-binding model.

*phewageegana1@gsu.edu
†vapalkov@gsu.edu

[1] K. S. Novoselov, A. K. Geim, S. V. Morozov, D. Jiang, Y. Zhang, S. V. Dubonos, I. V. Grigorieva, and A. A. Firsov, Science **306**, 666 (2004).
[2] K. S. Novoselov, A. K. Geim, S. V. Morozov, D. Jiang, M. I. Katsnelson, I. V. Grigorieva, S. V. Dubonos, and A. A. Firsov, Nature (London) **438**, 197 (2005).
[3] T. Ando, T. Nakanishi, and R. Saito, J. Phys. Soc. Jpn. **67**, 2857 (1998).
[4] M. I. Katsnelson, Mater. Today **10**, 20 (2007).
[5] T. Ando, in *Nanophysics & Bioelectronics: A New Odyssey*, edited by T. Chakraborty, F. Peeters, and U. Sivan (Elsevier, Amsterdam, 2002), Chap. 1.
[6] M. I. Katsnelson, K. S. Novoselov, and A. K. Geim, Nat. Phys. **2**, 620 (2006).
[7] O. Klein, Z. Phys. **53**, 157 (1929); Z. Phys. **41**, 407 (1927); A. Calogeracos and N. Dombey, Contemp. Phys. **40**, 313 (1999).
[8] T. Chakraborty, *Quantum Dots* (Elsevier, Amsterdam, 1999); T. Chakraborty, Comments Condens. Matter Phys. **16**, 35 (1992).
[9] H. Liu, M. Gao, J. McCaffrey, Z. R. Wasilewski, and S. Fafard, Appl. Phys. Lett. **78**, 79 (2001).
[10] D. Loss and D. P. DiVincenzo, Phys. Rev. A **57**, 120 (1998).
[11] V. V. Cheianov and V. I. Falko, Phys. Rev. B **74**, 041403(R) (2006).
[12] P. G. Silvestrov and K. B. Efetov, Phys. Rev. Lett. **98**, 016802 (2007).
[13] H.-Y. Chen, V. Apalkov, and T. Chakraborty, Phys. Rev. Lett. **98**, 186803 (2007).
[14] A. Matulis and F. M. Peeters, Phys. Rev. B **77**, 115423 (2008).
[15] P. Hewageegana and V. Apalkov, Phys. Rev. B **77**, 245426 (2008).
[16] D. Loss and D. P. DiVincenzo, Phys. Rev. A **57**, 120 (1998); A. Barenco, D. Deutsch, A. Ekert, and R. Jozsa, Phys. Rev. Lett. **74**, 4083 (1995); R. Landauer, Science **272**, 1914 (1996); J. A. Brum and P. Hawrylak, Superlattices Microstruct. **22**, 431 (1997).
[17] B. Trauzettel, D. V. Bulaev, D. Loss, and G. Burkard, Nat. Phys. **3**, 192 (2007).
[18] W. G. van der Wiel, S. De Franceschi, J. M. Elzerman, T. Fujisawa, S. Tarucha, and L. P. Kouwenhoven, Rev. Mod. Phys. **75**, 1 (2002).
[19] T. V. Shahbazyan and M. E. Raikh, Phys. Rev. B **49**, 17123 (1994).
[20] H.-Y. Chen, V. Apalkov, and T. Chakraborty, J. Phys.: Condens. Matter **20**, 135221 (2008).
[21] G. Gamow, Z. Phys. **51**, 204 (1928).
[22] M. L. Goldberger and K. M. Watson, *Collision Theory* (Wiley, New York, 1964).
[23] T. Ando, J. Phys. Soc. Jpn. **75**, 074716 (2006).
[24] R. Saito, G. Dresselhaus, and M. S. Dresselhaus, *Physical Properties of Carbon Nanotubes* (Imperial College Press, London, 1998).
[25] M. Ya. Azbel, Phys. Rev. B **28**, 4106 (1983); W. Xue and P. A. Lee, *ibid.* **38**, 3913 (1988).